BACE1 gene silencing alleviates isoflurane anesthesia-induced postoperative cognitive dysfunction in immature rats by activating the PI3K/Akt signaling pathway

YING-BIN WANG, JIAN-QIN XIE, WEI LIU, RONG-ZHI ZHANG, SHENG-HUI HUANG and YAN-HONG XING

Department of Anesthesiology, Lanzhou University Second Hospital, Lanzhou, Gansu 730030, P.R. China

Received October 31, 2017; Accepted August 1, 2018

DOI: 10.3892/mmr.2018.9453

Abstract. Postoperative cognitive dysfunction (POCD) is a severe complication characterized by cognitive dysfunction following anesthesia and surgery. The aim of the present study was to investigate the effects of β-site amyloid precursor protein cleavage enzyme 1 (BACE1) gene silencing on isoflurane anesthesia-induced POCD in immature rats via the phosphatidylinositol-3-kinase (PI3K)/protein kinase B (Akt) signaling pathway. Rat models were established and then transfected with BACE1 small interfering RNA and wortmannin (an inhibitor of PI3K). Blood gas analysis was performed, and a series of behavioral experiments were conducted to evaluate the cognitive function, learning ability and locomotor activity of rats. Reverse transcription quantitative polymerase chain reaction and western blot analysis were employed to determine the mRNA and protein expression of the associated genes. An ELISA was used to detect the inflammatory indicators and the content of amyloid precursor protein (APP) and amyloid-β (Aβ). Apoptosis of the hippocampal CA1 region was observed by terminal deoxynucleotidyl transferase dUTP nick-end labeling staining. Initially, it was revealed that the percentage of stagnation time in rats was increased by BACE1 gene silencing; the escape latency and swimming distance were markedly reduced from the 4th to the 6th day, the time the rats spent in first passing the target area was shortened, and the times of passing the target area were increased by BACE1 gene silencing, demonstrating that BACE1 gene silencing enhanced the spatial memory ability of rats. Additionally, it was determined that silencing BACE1 improved the pathological state induced by isoflurane anesthesia in immature rats, and attenuated the inflammatory response and the levels of APP and Aβ in hippocampal tissues. Furthermore, it was suggested that silencing BACE1 may have promoted the activation of the PI3K/Akt signaling pathway, thereby inhibiting the apoptosis of the hippocampal CA1 region. Taken together, these results indicated that BACE1 gene silencing may improve isoflurane anesthesia-induced POCD in immature rats by activating the PI3K/Akt signaling pathway and inhibiting the Aβ generated by APP.

Correspondence to: Professor Ying-Bin Wang, Department of Anesthesiology, Lanzhou University Second Hospital, 82 Cuiying Door, Chengguan, Lanzhou, Gansu 730030, P.R. China
E-mail: wangyingbin6@163.com

Key words: β-site amyloid precursor protein cleavage enzyme 1, gene silencing, phosphatidylinositol-3-kinase/protein kinase B signaling pathway, isoflurane anesthesia, amyloid precursor protein, β-amyloid, postoperative cognitive dysfunction

Introduction

Postoperative cognitive dysfunction (POCD) refers to an impactful decline in cognitive function that is commonly presented in older patients after surgery (1). The characteristics of POCD usually manifest as disorientation and impaired memory, concentration and thinking, but the etiology of POCD remains unclear (2,3). Moreover, there are various risk factors for POCD, including age, cognitive function before surgery, duration of the surgery, and respiratory complications and infection after surgery (4). Recently, POCD has been considered a serious problem affecting people's health and has an influence on both the outcome and elevated costs of patients, but until now, only a few useful treatments have been discovered (5). POCD can last for several days or even several years; consequently, the quality of life of the patients is extremely disrupted, there is an increase in hospitalization and in extra hospital nursing expenses, and POCD is also blamed for increasing morbidity and mortality during surgery (2). According to previous, efficient studies, it is suggested that the regulation of certain signaling pathways are implicated in POCD (3,6-8).

Calcium regulation [such as phosphatidylinositol 3-kinase (PI3K) pathway] is closely related to neurodegenerative diseases such as POCD (9). According to Hu *et al* (10), the inhibition of PI3K is partially involved in different stages of POCD, but the exact mechanism is not clear. There are several articles about the negative regulation between BACE1 and PI3K activation (11,12), but the specific molecular mechanism is not clarified. The protein kinase B (Akt) signaling pathway is considered one of the potential mechanisms in the progression of POCD, and the expression of the β-site amyloid precursor protein cleavage enzyme 1 (BACE1) gene is downregulated by activating the PI3K/Akt pathway (6,12). It has been demonstrated that deregulation of the PI3K pathway is associated

with prostate cancer and that myocardial viability is partially improved by activation of the PI3K/Akt pathway (13,14). Amyloid-β (Aβ) protein, a major factor causing neuritic plaques in the brains of Alzheimer's disease (AD) patients, is generated by BACE1 (15). Genetic studies have found an important relationship between Aβ and neurodegenerative diseases, and Aβ involves several pathways, such as PI3K and C-Jun, involved in the development of the disease (16,17). Besides, Aβ promotes the production of reactive oxygen species (ROS) and induces neuronal apoptosis, and activation of iNOS pathway induces neurotoxicity; Aβ upregulates intracellular calcium concentration to regulate synaptic plasticity of dendritic cells (16,17). However, the different size of Aβ peptide region and the different biological process of the involved pathway regulation lead to the unknown mechanism of Aβ in disease (18,19). It has been proven that an increased BACE1 level elevates Aβ production and plays a role in promoting AD (20). Moreover, BACE1 is a main target to modify the treatment for AD, and by inhibiting BACE1 expression, AD can be relieved and even prevented through inhibiting the expression of BACE1 (21,22). These evidences suggest that BACE1 might participate in the POCD process by mediating the production of Aβ and regulating the PI3K pathway. Therefore, the present paper aims to analyze the effects of BACE1 gene silencing in rats with POCD through the PI3K/Akt pathway, which will potentially provide an extra option for POCD treatment.

Materials and methods

Model establishment. A total of 120 7-day-old male Sprague-Dawley (SD) rats with a weight of 15 to 20 g were purchased from the Experimental Animal Center of Lanzhou University Second Hospital. Twenty rats without any treatment were enrolled in the control group, and the remaining rats were placed in an organic glass box (20x40x15 cm) and included in the model group. The inlet and exhaust ports were at opposite sides of the box. A Vapor 2000 Anesthetic Vaporizer (Draeger Medical Equipment Co., Ltd., Shanghai, China) was attached to the inlet port to infuse oxygen and isoflurane, and the 5250 Respiratory Gas Monitor (Ohmeda, Louisville, CO, USA) was connected with the exhaust port to detect the concentration of oxygen, isoflurane and carbon dioxide. An electric heating blanket was placed on the bottom of the box to keep the rats' body temperature at 38 to 39˚C. The rats in the control group inhaled pure oxygen for 4 h at a flow rate of 4 l/min. The rats in the model group inhaled isoflurane for 4 h, and the concentration of isoflurane was 3.4 to 3.6% in 1 h, 2.1 to 2.3% after 1 h and 1.7 to 1.8% after 2 to 4 h. The loss of a righting reflex in the rats was considered the onset of anesthesia. All the animal experiments in the study were in accordance with the Guide for the Care and Use of Laboratory Animals (23) issued by the National Institutes of Health.

BACE1 siRNA vector construction and grouping. The small interfering RNA (siRNA) of BACE1 was synthesized using the *in vitro* transcription method. The complete sequence of BACE1 mRNA in rats was obtained from GenBank (GenBank accession no. NM012104). The target sequence of siRNA was 5'-GACGCUCAACAUCCUGGUG-3'. According to the design principles for short hairpin RNA (shRNA), a loop region, reverse complementary sequence and transcription terminator were added to the sequence above for the transcription of shRNA. Restriction enzyme sites Sal I (GTCGAC), Hind III (AAGCTT) and Xho I (CTCGAG) and protective bases were also added to the cloned fragments to obtain a more efficient insertion into the vector. In addition, the single-stranded DNA of BACE1 siRNA was obtained. The synthesized single-stranded DNA was diluted to 20 pmol/l with sterile water, and double-stranded DNA was obtained after annealing. The product after annealing was connected to the linearized vector. *Escherichia coli* DH5α was transformed, applied on flat plates, and cultured overnight at 37˚C. Two colonies were selected with sterile toothpicks from each plate corresponding to each sequence, lysed for 10 min at 95˚C, and added into the reverse transcription-quantitative polymerase chain reaction (RT-qPCR) system with the primers of multiple cloning sites in the vectors. A total of 5 μl of PCR product was obtained and analyzed by 2% agarose gel electrophoresis to select the positive colonies. In addition, the plasmid DNA was then extracted, and the sequences were analyzed. The endotoxin-free DNA was extracted from the transformed strain corresponding to the recombinant expression vector with the identified correct sequence in strict accordance with the instructions of the Plasmid Maxi Preparation kit (Shanghai Yanhui Biotech Co., Ltd., Shanghai, China). After the successful construction of the recombinant vector, the BACE1 siRNA plasmid and blank plasmid were extracted and diluted to 0.1 to 3 μg/μl with interventions to the rats on the first day after successful modeling. In addition, 80 rats from the model group were equally divided into 4 groups, as follows: (1) The si-BACE1 group: 10 μl of BACE1 siRNA plasmid DNA solution was injected through the caudal vein. (2) The wortmannin group: PI3K inhibitor wortmannin (S2758; Selleck Chemicals, Houston, TX, USA) at a concentration of 2 mg/kg was injected through the caudal vein 30 min before anesthesia, and the model was established with the same method described above. (3) The negative control (NC) group: A total of 10 μl blank plasmid without siRNA was transfected. (4) The si-BACE1 + wortmannin group: PI3K inhibitor wortmannin (S2758; Selleck Chemicals) at a concentration of 2 mg/kg was injected through the caudal vein 30 min before anesthesia; the model was established with the same method described above, and 10 μl BACE1 siRNA plasmid DNA solution was injected through the caudal vein after modeling. At the same time, the rats in the control group and model group were all injected with the same dosage of saline once a day for 7 days.

Blood gas analysis. Four h after transfection, 200 μl of blood was extracted from the left ventricle of the rats in each group, and an I-STAT portable blood gas analyzer (Boyu Medical Equipment Co., Ltd., Shanghai, China) was applied to measure the blood glucose level, pH, PaO_2 and $PaCO_2$.

Spontaneous locomotor activity test. A ZZ-6 autonomic activity tester purchased from the Beijing Institute of Respiratory Medicine (Beijing, China) was applied to test the locomotor activity. The box was made of 4 black opaque sealed cylinders with a diameter of 50 cm and a height of 40 cm containing 4 phototubes on the inner surface to record the locomotion of rats. During the experiment, the rats were gently

placed in the box, and the lid was closed. The duration of each test was 10 min, and the test was performed daily for 5 days. The equipment was cleaned with water to prevent odors from interfering with the judgment of the rats after each experiment. The room was kept quiet before and after the experiment, and the temperature was kept constant at 24˚C.

Fear conditioning test. Fear conditioning was measured to evaluate the cognitive function of rats using the fear conditioning analysis system (XR.XC404; Shanghai Xinruan Information Technology Co., Ltd., Shanghai, China). On the first day, sound stimulation (2000 Hz, 90 dB, 30 sec) was conducted after 3 min of an adaptive phase, and electric current stimulation (1 mA, 2 sec) started at the last 2 sec of sound stimulation and ended at the same time as the sound stimulation, with an interval of 1 min. On the second day, cued and contextual fear conditioning experiments were conducted. For the contextual conditioning, the rats were placed in the same scene on the first day without sound or electric current stimulation and recorded for 8 min. For the cued conditioning, the rats were placed in a different scene from the first day, and after 3 min of the adaptive phase, sound stimulation (2000 Hz, 90 dB, 30 sec) was released 3 times with an interval of 1 min without an electric current and recorded for 8 min. Image analysis software (Shenzhen RWD Life Science Co., Ltd., Shenzhen, China) was used to calculate the percentage of stagnation time of the rats in cued and contextual fear conditioning.

Morris water maze test. A water maze (Chinese Academy of Medical Sciences, Beijing, China) was adopted with a diameter of 214 cm, a height of 50 cm, a depth of 30 cm and a black bottom. At the beginning of the experiment, Chinese ink was dropped into the water to darken the water. Four white spots were marked in equidistance counter-clockwise on the wall of the pool. The four quadrants of the pool were west, south, east and north, and a circular platform (10 cm in diameter and 28 cm in height) was placed in the north quadrant. A camera was installed right above the pool with a clear vision of the entire water maze. The experiment was conducted in a quiet room with artificial lighting. During the experiment, the water temperature was 20 to 23˚C, and the water was changed every day. The rats were fasted for 4 h before the experiment, and their fur was dried after the experiment. A week after the drug injection, the rats were pretrained 3 times a day (with an interval of 2 h each time) for 2 days. During the training, the rats were randomly put in different quadrants of the pool with their heads against the wall. The rats were guided to swim in a straight line toward the platform and to stay on the platform for 30 sec.

For the orientation navigation experiment, the rats were put into the water from different quadrants, each time with their heads against the wall. When the rats entered the water, the escape latency and swim distance were recorded. A Morris water maze was performed in 15 rats of each group. The time period between the rats getting into the water and finding the platform was defined as the escape latency. The rats that could not find the platform in 60 sec were placed on the platform for 10 sec, and the escape latency was recorded as 60 sec. The training was performed 4 times a day for 5 days, and the locations of water entry were randomly chosen in different quadrants every time. The average value of the entire experiments was regarded as the ability of learning and memory, and the escape latency represented the spatial learning ability of rats. For the space exploration experiment, the platform was removed the next day after the orientation navigation experiment. The rats were put into the water from the contralateral quadrant of the previous quadrant of the original platform. The swimming trace for 120 sec, the time when the rats first reached the platform and the number of times that the rats passed the target area within 120 sec was recorded to reflect the spatial learning ability of the rats. After comparison and analysis, the memory ability of rats to find the original platform was investigated. If the rats did not pass the target area in 120 sec, then the time was recorded as 120 sec, and the number of passing times was 0. The data collection and processing were accomplished by the Morris software.

RT-qPCR. After the behavioral experiments, the rats in each group were sacrificed, the skulls were opened, and the brain tissues were taken out, frozen immediately by liquid nitrogen and stored at -80˚C in a refrigerator. The total RNA was extracted from brain tissues according to the instructions of the kit (Shanghai Yanhui Biotech Co., Ltd.). The RNA was reversely transcribed into cDNA. The total volume of the PCR reaction was 10 μl, including 1 μl of cDNA, 5 μl of 2X SYBR® Premix Ex Taq XmlI, 0.4 μl of forward primer, 0.4 μl of reverse primer, and 3.2 μl of double distilled water. The conditions were 2 min of predenaturation at 94˚C, 30 cycles of 45 sec at 94˚C, 45 sec at 55˚C and 1 min at 72˚C, and a final extension for 10 min at 72˚C. GAPDH served as an internal reference. The primer sequences are shown in Table I. PCR products were detected by 2% agarose gel electrophoresis. The integrated optical density (OD) was calculated as the gray value multiplying the area. The relative gene expression was represented by the $2^{-\Delta\Delta Cq}$ method and the ratio of integrated OD of the target gene to the reference gene (24). In addition, ΔCq represented the difference between the Cq value of the target gene and the Cq value of the reference gene (25). RT-qPCR was also used to detect the mRNA expression of caspase-3 and PI3K/Akt signaling pathway-related genes.

Western blot analysis. Brain tissues were added to a protein extraction reagent (Beijing Biolab Technology Co., Ltd., Beijing, China) according to a 1: 10 (g/l) ratio. The components of the reagent were 20 mM Tris (pH, 7.5), 150 mM NaCl, 1% Triton X-100, Na2HPO4, β-glycerophosphate, ethylenediamine tetraacetic acid (EDTA), Na3VO4, PVP40 and leupeptin. The extracted protein was centrifuged at 12,500 rpm for 15 min to obtain the supernatant, and the protein was quantitatively determined by the bicinchoninic acid (BCA) kit (Beyotime Institute of Biotechnology, Jiangsu, China). A sample with the same amount of the protein was taken and diluted to 20 μl with 4x loading buffer and normal saline. After denaturation at 100˚C for 5 min, sodium dodecyl sulfate-polyacrylamide gel electrophoresis (SDS-PAGE) was prepared according to the relative molecular weight of the target protein. The proteins were transferred onto the membrane according to the concentration and loading quantity of the protein. Five percent skim milk was used to block the membrane for 1 h. After gently shaking at

Table I. Primer sequences for reverse transcription-quantitative polymerase chain reaction.

Gene	Forward primer sequence (5'-3')	Reverse primer sequence (5'-3')
BACE1 (NM012104)	TGGTGGACACGGGCAGTAGTAA	TCGGAGGTCTCGGTATGTACTGG
Caspase-3 (NM012922)	TACCCTGAAATGGGCTTGTGT	GTTAACACGAGTGAGGATGTG
PI3K (NM053481)	TGGACGGCGAAGTAAAGCATT	AGTGTGACATTGAGGGAGTCG
Akt (NM033230)	CTCATTCCAGACCCACGAC	ACAGCCCGAAGTCCGTTA
GAPDH (NM017008)	GACAACTTTGGCATCGTGGA	ATGCAGGGATGATGTTCTGG

BACE1, β-site amyloid precursor protein cleavage enzyme 1; PI3K, phosphatidylinositol 3-kinase; Akt, protein kinase B.

37˚C for 2 h, GAPDH (ab9485, 1:5,000) and the primary antibodies BACE1 (ab108394, 1:1,000), PI3K (ab86714, 1:1,000), phosphorylated (p)-PI3K (ab182651, 1:1,000), Akt (ab8805, 1:500), p-Akt (ab8933, 1:1,000), caspase-3 (ab13847, 1:500) and cleaved-caspase-3 (ab49822, 1:500; all purchased from Abcam, Cambridge, MA, USA) were added for incubation at 4˚C overnight. The membrane was washed 3 times, each time for 5 min. POD-conjugated goat anti-rabbit antibody (A5795, 1:5,000; Sigma-Aldrich; Merck KGaA, Darmstadt, Germany) was added to incubate for 1.5 h at 37˚C, and the membrane was washed 3 times for 10 min each time. Luminescent reagent was added, and the film was exposed by X-ray, developed and fixed in the darkroom. Quantity One software was employed for the semiquantitative analysis for BACE1 expression. The ratio of the gray value of the internal reference to that of BACE1 on film represented the expression level of BACE1. This method was also applied to detect the protein expression of caspase-3 and PI3K/Akt signaling pathway-related genes.

Hematoxylin and eosin (HE) staining. The brain tissues were removed, and the hippocampus of one side of the cerebral hemisphere was separated on the ice, immediately frozen by liquid nitrogen and stored at -80˚C in the refrigerator. The other side of the cerebral hemisphere was fixed in a 500 ml mixture of 2% paraformaldehyde and 2% glutaraldehyde at 4˚C for 2 h, and the brain was then removed and soaked in a freshly mixed fixative solution at 4˚C for 12 h. The hippocampus was separated the next day. The tissues in the hippocampal CA1 region were paraffin-embedded, and serial coronal sections (4 mm) were cut behind the optic chiasm. The sections were baked at 60˚C overnight and dewaxed in xylene I and xylene II for 20 min. The sections were placed into 100, 95, 80 and 70% ethanol for 5 min respectively, stained by hematoxylin for 10 min, and rinsed by running water for 15 min. Eosin was used to stain the sections for 30 sec, and double distilled water was used to wash the sections. After the sections were dehydrated by ethanol, cleared in xylene and sealed with neutral balsam, the ultrastructure and number of pyramidal cells in the hippocampal CA1 area were observed and photographed using an electron microscope.

TUNEL staining. Using the same method of HE staining, hippocampal CA1 tissues of rats were treated by TUNEL staining. Then, they were cut into sections, and later, these tissues were dewaxed in xylene I and II for 20 min and then were placed in 100, 100, 95, 80 and 70% ethanol for 5 min separately. After washing with phosphate buffered saline (PBS) twice (5 min each time), the tissues were fixed in 4% paraformaldehyde for 15 min. After again washing twice with PBS (5 min each time), then 100 μl proteinase K (20 μg/ml) was added to each section. After being treated at room temperature for 15 min, the tissues were twice washed in PBS (for 5 min each). Then, the TUNEL kit of Promega Corporation (Madison, WI, USA; cat. no. G3250) was used for staining. The specific steps were in line with the instructions. After adding 100 μl equilibrium liquid, the tissues were put in a wet box for balance for 10 min. The TUNEL reaction mixture was made as follows: the treatment group was mixed with 1 μl rTdT+1 μl biotin-labeled dUTP + 98 μl equilibrium liquid, and the negative control group was mixed with three-fold-distilled water rather than rTdT. In the positive control group, the tissues were incubated after adding 100 μl DNase 1 buffer for 5 min. After removing the liquid, the tissues were enzymatically digested by adding 100 μl DNase 1 (10 U/ml) for 10 min. After washing with deionized water 4 times and with PBS for 5 min, 100 μl TUNEL reaction mixture was added to the sample. Then, the sample was placed in a dark wet box after being covered by a cover glass or sealing film for reaction at 37˚C x 1 h. The TUNEL reaction was stopped after the sample was immersed in 2x SSC for 15 min. After being washed in PBS 3 times (5 min for each), the sample was closed in peroxidase (POD), immersed in 0.3% H2O2 for 15 min, and then again immersed for washing 3 times with PBS (for 5 min each). The sample was mixed with 100 μl streptavidin-labeled HRP (diluted based on 1:500 of PBS) for a 30 min reaction and immersed by again washing 3 times with PBS (for 5 min each). Subsequently, 100 μl DAB mixture (50 μl DAB + 50 μl DAB substrate buffer + 50 μl H2O220 x + 950 μl threefold-distilled water) was supplemented for a 10 min reaction. When a light brown background appeared under the microscope, the sample was rinsed with deionized water and redyed with hematoxylin for 3 sec. Then, the sample was immediately washed with running water. After being dehydrated by gradient alcohol (50, 70, 85, 95, 100, 100%, 1 min for each) and cleared by xylene II, the sample was mounted by neutral balata. Finally, the positive apoptotic cells were observed under a microscope, with 10 pictures taken in each group to determine the apoptosis rate of positive cells in the hippocampal CA1 region.

Enzyme-linked immunosorbent assay (ELISA). The other side of the frozen hippocampus (approximately 100 mg) was homogenized and centrifuged, and then the supernatant was extracted

according to the instructions of the ELISA kits for TNF-α, IL-1, IL-6, Aβ and amyloid precursor protein (APP) purchased from Shanghai Westang Biotech Co., Ltd., (Shanghai, China). The kits were placed at room temperature for 20 min, and the washing solution was prepared. A total of 10 standard wells were arranged on the ELISA plate, including 2 blank wells without samples or ELISA reagents. The standard solution was subjected to gradient dilution, and the standard curve was created. The sample was diluted 10-fold with normal saline and then added to the wells of the ELISA plate. The plate was gently shaken and incubated at 37˚C for 30 min after being sealed. The liquid in the wells was removed, and the washing solution was added and then removed after 30 sec, and the step was repeated 5 times before drying the plate. In addition, 50 μl of ELISA reagent was added and incubated at 37˚C for 30 min, and the liquid in the wells was removed. The washing solution was added and then removed after 30 sec, and the step was repeated 5 times before drying the plate. Next, 50 μl of chromogenic reagent A and 50 μl of chromogenic reagent B was added to each well and incubated at 37˚C for 15 min in the dark after shaking, followed by the addition of 50 μl stop solution. The microplate reader (Bio-Rad, Hercules, CA, USA) was applied to measure the OD value (450 nm) of each well at 10 min. The concentration standard curve was drawn with the OD value as the vertical coordinate and the standard solution as the horizontal coordinate. According to the OD value, the concentration of the sample was determined and recorded.

Statistical analysis. SPSS v.22.0 software (IBM Corp., Armonk, NY, USA) was used for statistical analysis. All tests were repeated three times, and the means and standard deviations were calculated. Measurement data are expressed as the mean ± standard deviation. The comparison between groups was conducted by one-way analysis of variance, which was combined with Tukey's Honest Significant Difference post hoc test, and repeated measures analysis of variance combined with the Bonferroni post hoc test was used to analyze the differences in a group at different time points. P<0.05 was considered to indicate a statistically significant difference.

Results

No hypoxia or carbon dioxide accumulation were found in each group. Measurement of the arterial blood gas index and blood glucose was carried out. The results showed that among the rats of 6 groups, all the pH values were in the normal range without hypoxia or carbon dioxide accumulation in each group. The pH, *Pa*O_2, *Pa*CO_2 and blood glucose level had no significant difference, as shown in Table II (all P>0.05).

The spontaneous locomotor activity and standing up of rats exhibited no significant differences among the six groups. According to the results of experiments on the spontaneous locomotor and standing activities of rats (Fig. 1), no significant differences were found in the standing and locomotor activities of rats in each group (all P>0.05).

BACE1 gene silencing increased the percentage of stagnation time in the fear conditioning test of rats . The contextual fear conditioning test was performed for observing the percentage of stagnation time of rats. Its results indicated that compared with the control group, the model, NC, si-BACE1 + wortmannin and wortmannin groups had a lower percentage of stagnation time (all P<0.05). The percentage of stagnation time in the si-BACE1 group was significantly higher than that in the model group (P<0.05), while the percentage of stagnation time in the wortmannin group was remarkably lower than that in the model group and si-BACE1 + wortmannin group (all P<0.05). There were no significant differences in the percentage of stagnation time among the si-BACE1 + wortmannin, model and NC groups (all P>0.05). In the cued fear conditioning test, the percentage of stagnation time was not significantly different in the 6 groups (all P>0.05, Fig. 2). Consequently, the results of the study confirmed that the percentage of stagnation time of rats can be increased by BACE1 gene silencing.

BACE1 silencing enhanced the spatial memory ability of rats. Several experiments were carried out to measure the spatial memory ability of rats. The escape latency and swimming distance of rats in the control group and si-BACE1 group decreased significantly during the 5-day training. However, the escape latency and the swimming distance were longer and decreased slowly in the model, NC, si-BACE1 + wortmannin and wortmannin groups compared to the control group during the fourth to sixth day (P<0.05). On the seventh day of the space exploration experiment, in comparison to the control group, the model, NC and si-BACE1 + wortmannin groups spent more time to first pass the target area and passed the target area remarkably fewer times (all P<0.05). Compared to the model group, the escape latency and swimming distance was obviously reduced from the fourth to the sixth day, the time that the rats spent in first passing the target area shortened, and the times of passing the target area rose in the si-BACE1 group. However, when compared to the model and si-BACE1 + wortmannin group, the wortmannin group had a significantly longer escape latency and swimming distance from the fourth to sixth day, and the time the rats spent in first passing the target area extended and the times of passing the target area reduced (all P<0.05). In addition, there was no significant difference in the escape latency, swimming distance and exploration time among the model group, NC group and si-BACE1 + wortmannin group (all P>0.05, Fig. 3). In brief, the findings verified that BACE1 gene silencing enhances the spatial memory ability of rats.

mRNA and protein expression of BACE1 was the highest in the wortmannin group. RT-qPCR results showed that compared with the control group, the expression of BACE1 in rats in the model, NC and wortmannin groups was upregulated. In addition, the expression in the si-BACE1 group and si-BACE1 + wortmannin group was lower than that in the model group. The expression of BACE1 in the wortmannin group was higher than that in the model group (P<0.05). There was no significant difference between the NC and model groups (P>0.05) (Fig. 4A), and the results of western blot analysis detection of protein were consistent with those of RT-qPCR (Fig. 4B and C).

Silencing BACE1 improved the pathological state of immature rats induced by isoflurane anesthesia. Isoflurane anesthesia

Table II. Blood gas indices and blood glucose levels in the rat artery among the six groups.

Group	pH	$PaCO_2$ (mmHg)	PaO_2 (mmHg)	Blood glucose (mmol/l)
Control	7.88±0.12	37.81±5.11	105.21±6.40	5.14±0.82
Model	7.73±0.17	39.47±4.30	100.24±8.30	4.84±0.75
NC	7.84±0.23	38.62±4.62	102.63±5.64	4.64±0.60
Si-BACE1	7.78±0.16	39.33±5.20	101.53±7.30	4.05±0.70
Si-BACE1 + wortmannin	7.90±0.25	38.93±4.80	103.15±6.50	4.93±0.55
Wortmannin	7.80±0.27	38.12±4.04	102.85±6.70	4.75±0.96

NC, negative control; si, small interfering; BACE1, β-site amyloid precursor protein cleavage enzyme 1; Pa, partial pressure.

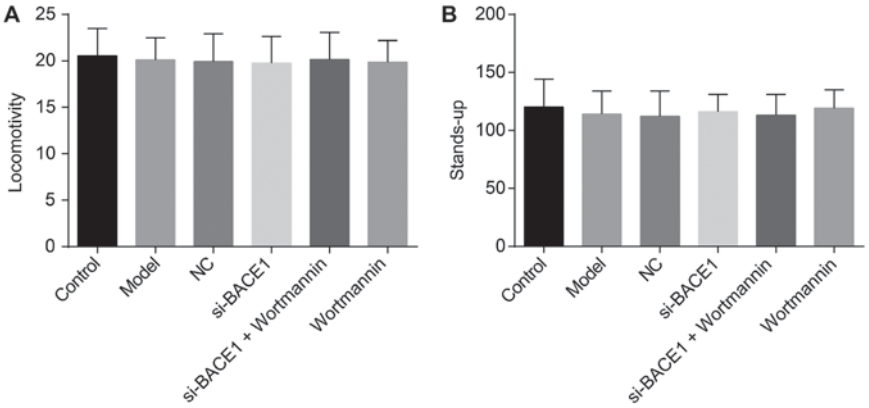

Figure 1. Locomotivity and standing actions. The results revealed that there was no significant difference in the locomotor and standing activities of rats. (A) The number of locomotive actions of rats in the six groups. (B) The number of standing actions of rats in the six groups. NC, negative control; si-, small interfering RNA; BACE1, β-site amyloid precursor protein cleavage enzyme 1.

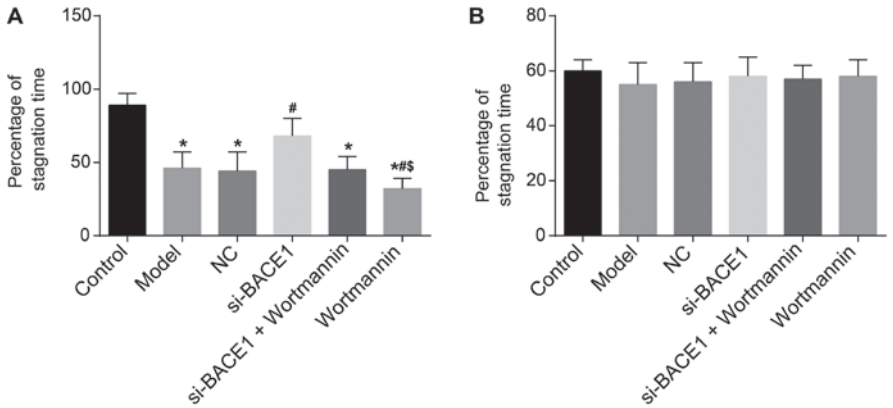

Figure 2. Fear conditioning tests. The results revealed that silencing of BACE1 elevated the percentage of stagnation time. (A) Silencing BACE1 increased the percentage of stagnation time in contextual fear conditioning among the six groups. (B) There was no significant difference in the percentage of stagnation time in each group in the cued fear conditioning test. *P<0.05 vs. the control group; $^{\#}$P<0.05 vs. the model group; $^{\$}$P<0.05 vs. the si-BACE1 + wortmannin group. NC, negative control; si-, small interfering RNA; BACE1, β-site amyloid precursor protein cleavage enzyme 1.

was performed, and its results showed that the intensively stained hippocampal pyramidal cells were annular. The hippocampal CA1 neurons in the control group were regularly arranged, and the cells were morphologically normal and orderly arranged. The neurons were of similar size with clear structures of mitochondria and synapse. The synapses were evenly distributed, the presynaptic and postsynaptic membranes were close, and the synaptic vesicles were abundant and concentrated. The hippocampal CA1 neurons in the model, NC and si-BACE1 + wortmannin groups were irregularly arranged, without a clear structure of mitochondria. The synaptic vesicles were reduced and scattered, and the presynaptic and postsynaptic membranes were not clear. The synaptic cleft widened, and the synaptic vesicles were sparsely distributed. The nuclei were intensively stained with karyopyknosis and dissolution, and there was vacuolization in

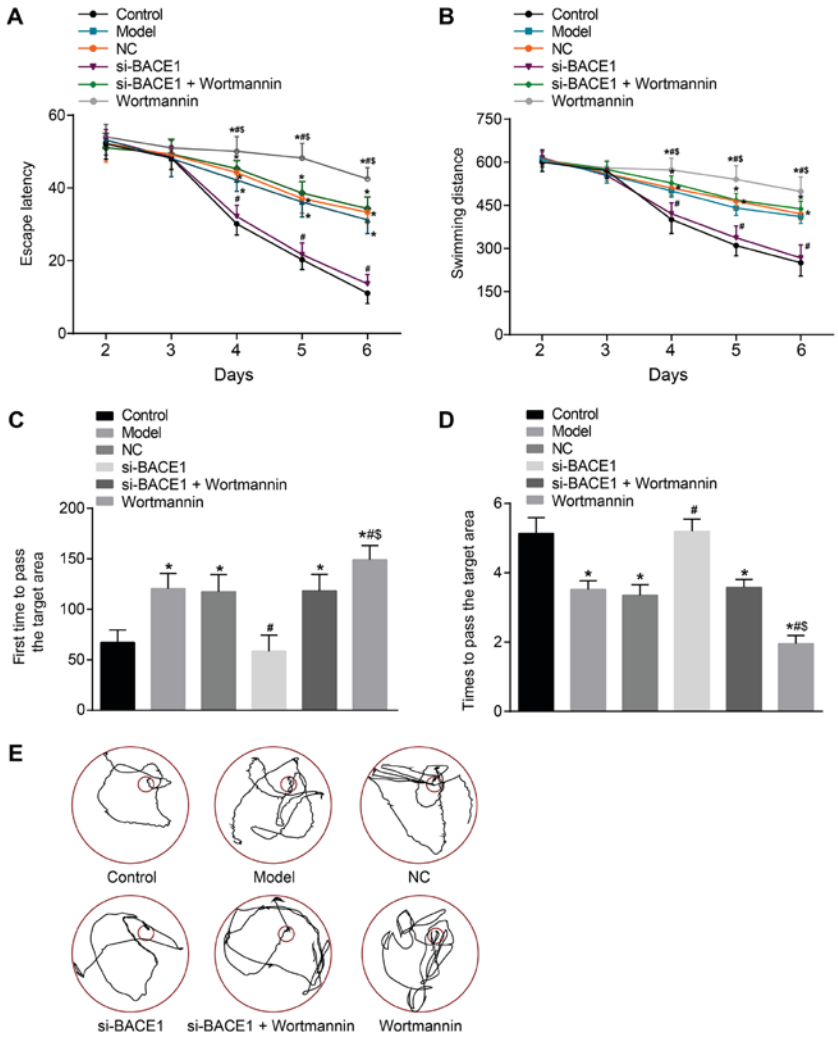

Figure 3. BACE1 silencing enhances the spatial memory ability of rats by the Morris water maze test. (A) The escape latency and (B) swimming distance were markedly reduced from the 4th to 6th day by silencing BACE1. (C) The time that the rats spent in first passing the target area shortened, and (D) the times of passing the target area rose by silencing BACE1. (E) Morris water maze test. *P<0.05 vs. the control group; #P<0.05 vs. the model group; $P<0.05 vs. the si-BACE1 + wortmannin group. NC, negative control; si-, small interfering RNA; BACE1, β-site amyloid precursor protein cleavage enzyme 1.

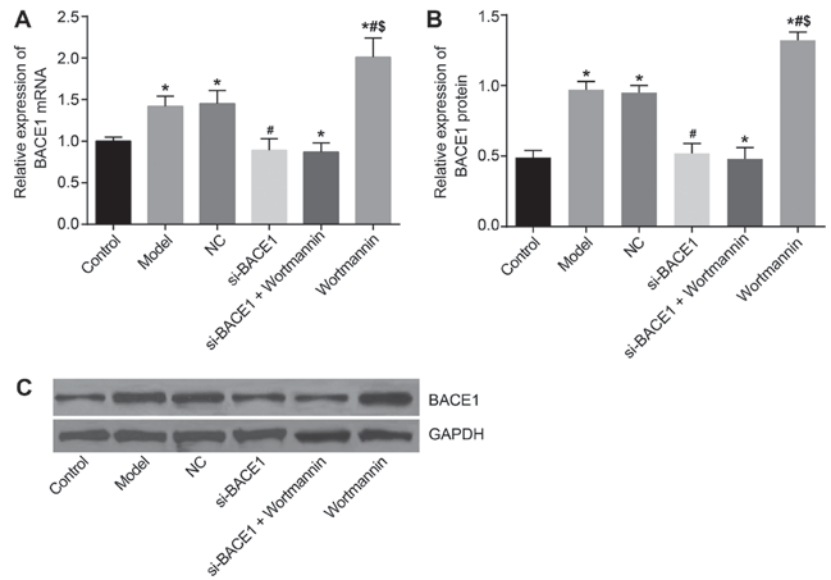

Figure 4. mRNA and protein expression of BACE1 is the highest in the wortmannin group. (A) The expression of BACE1 mRNA was the greatest in the wortmannin group following reverse transcription-quantitative polymerase chain reaction. (B) The expression of BACE1 protein was the highest in the wortmannin group, (C) as determined by western blot analysis. *P<0.05 vs. the control group; #P<0.05 vs. the model group; $P<0.05 vs. the si-BACE1 + wortmannin group. NC, negative control; si-, small interfering RNA; BACE1, β-site amyloid precursor protein cleavage enzyme 1.

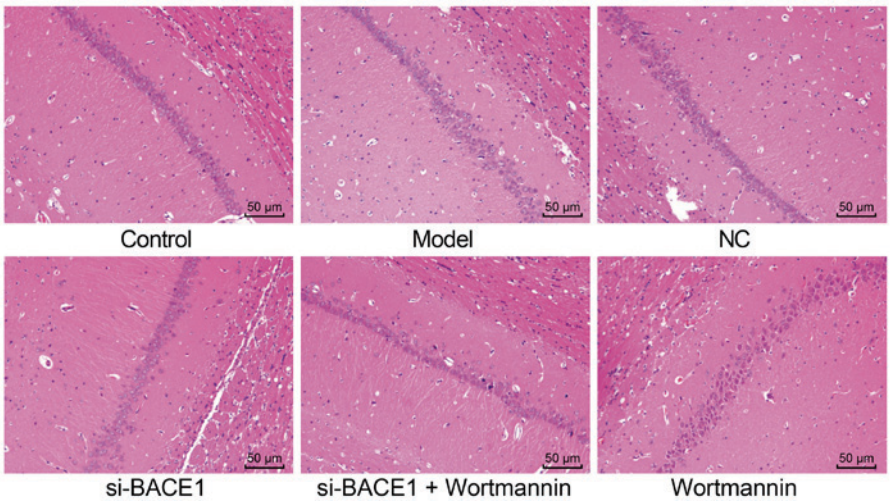

Figure 5. Silencing BACE1 improved the pathological state of immature rats induced by isoflurane anesthesia (magnification, x200; scale bars, 50 μm). NC, negative control; si-, small interfering RNA; BACE1, β-site amyloid precursor protein cleavage enzyme 1.

some neurons. In the si-BACE1 group, the hippocampal CA1 neurons were rather regularly arranged, with a clear structure of mitochondria. The synapses were evenly distributed, and the presynaptic and postsynaptic membranes were rather close, with relatively close synaptic vesicles. There was less pathological damage in the si-BACE1 group compared to the model group, but the pathological damage in the wortmannin group worsened compared to that in the model and si-BACE1 + wortmannin groups (Fig. 5). Taken together, silencing BACE1 improves the pathological state of immature rats induced by isoflurane anesthesia.

BACE1 gene silencing decreased TNF-α, IL-1β, IL-6, APP and Aβ levels in the rat hippocampus. Next, TNF-α, IL-1β, IL-6, APP and Aβ levels in the rat hippocampi among the six groups were detected. The TNF-α level in the hippocampus was similar among the 6 groups (all P>0.05). Compared to the control group, the hippocampal IL-1β, IL-6, APP and Aβ levels in the model, NC, si-BACE1 + wortmannin and wortmannin groups were remarkably elevated (all P<0.05). The hippocampal IL-1β, IL-6, APP and Aβ levels in the si-BACE1 group were notably lower than those in the model group (all P<0.05). The levels of IL-1β, IL-6, APP and Aβ in the wortmannin group were significantly higher than those in the si-BACE1 + wortmannin and model groups (all P<0.05). No differences were noted among the model, NC and si-BACE1 + wortmannin groups or between the si-BACE1 and control groups (all P>0.05, Table III). These results suggested that silencing BACE1 attenuates the inflammatory response and the levels of APP and Aβ in hippocampal tissues.

BACE1 gene silencing activated the PI3K/Akt signaling pathway. RT-qPCR was used to detect the mRNA expression of related genes. The results revealed that the PI3K and Akt mRNA expression levels in the hippocampus among the model, NC, si-BACE1 + wortmannin and wortmannin groups exhibited a notable decrease, while the mRNA expression of caspase-3 remarkably increased in comparison to the control group (all P<0.05). Compared to the model and NC groups, the relative mRNA expression levels of PI3K and Akt in the si-BACE1 group were significantly elevated, but the mRNA expression of caspase-3 was reduced (all P<0.05); the relative mRNA expression levels of PI3K and Akt were significantly lower but the mRNA expression level of caspase-3 was remarkably higher in the wortmannin group than in the si-BACE1 + wortmannin group (all P<0.05). The mRNA expression levels of PI3K and Akt in the wortmannin group were lower and the caspase-3 protein expression level was significantly higher than those in the si-BACE1 + wortmannin group (all P<0.05). The results of western blot analysis demonstrated that the protein expression levels of PI3K and Akt and the extent of PI3K and Akt phosphorylation in the model, NC, si-BACE1 + wortmannin and wortmannin groups declined, while the protein expression level of caspase-3 obviously increased compared to that in the control group (all P<0.05). However, the si-BACE1 group and control group exhibited no significant difference (P>0.05). The protein expression levels of p-PI3K/PI3K and p-AKT/AKT in the si-BACE1 group were higher, and the cleaved-caspase-3/caspase-3 expression level decreased notably compared with the levels in the model and NC groups (all P<0.05), and the wortmannin group showed the opposite tendency. The protein expression levels of PI3K and Akt and the extent of PI3K and Akt phosphorylation in the wortmannin group were lower than those in the si-BACE1 + wortmannin group, and the caspase-3 protein expression level was significantly higher (all P<0.05). The PI3K, Akt and caspase-3 expression levels in the model, NC and si-BACE1 + wortmannin groups exhibited no significant difference (all P>0.05, Fig. 6). All these results indicated that BACE1 gene silencing activates the PI3K/AKT signaling pathway.

Silencing BACE1 promoted the activation of the PI3K/Akt signaling pathway, thereby inhibiting the apoptosis of the hippocampal CA1 region. To further prove that increased expression of caspase3 induced cell apoptosis in the hippocampal CA1 region of rats, we performed TUNEL staining. The results showed that in the model, NC, si-BACE1 + wortmannin and wortmannin groups, the positive rate of TUNEL staining in rat hippocampus CA1 was significantly higher than that in the control group. Compared with the model and

Table III. TNF-α, IL-1β, IL-6, APP and Aβ levels in the rat hippocampus of the six groups.

Group	TNF-α (pg/g)	IL-1β (pg/g)	IL-6 (pg/g)	APP	Aβ
Control	130.23±18.07	108.03±16.12	47.24±7.06	10.04±3.45	205.24±19.45
Model	134.12±16.06	169.45±19.04[a]	84.24±9.12[a]	25.67±4.02[a]	390.74±15.06[a]
NC	132.14±14.73	166.54±20.34[a]	82.32±6.67[a]	26.78±3.46[a]	387.19±16.09[a]
si-BACE1	129.35±15.09	120.78±18.02[b]	52.35±5.35[b]	9.76±2.67[b]	210.36±10.92[b]
si-BACE1 + wortmannin	136.78±17.07	168.65±21.02[a]	80.76±7.14[a]	24.9 0± 2.26[a]	396.54±13.67[a]
Wortmannin	133.67±12.08	192.08±22.12[a-c]	104.21±9.45[a-c]	44.32±5.34[a-c]	450.45±20.09[a-c]

[a]P<0.05 vs. control; [b]P<0.05 vs. model; [c]P<0.05 vs. si-BACE1 + wortmannin group. BACE1, β-site amyloid precursor protein cleavage enzyme 1; NC, negative control; si, small interfering; APP, β-amyloid precursor protein; Aβ, β-amyloid; TNF-α, tumor necrosis factor-α; IL-1β, interleukin-1β; IL-6, interleukin-6.

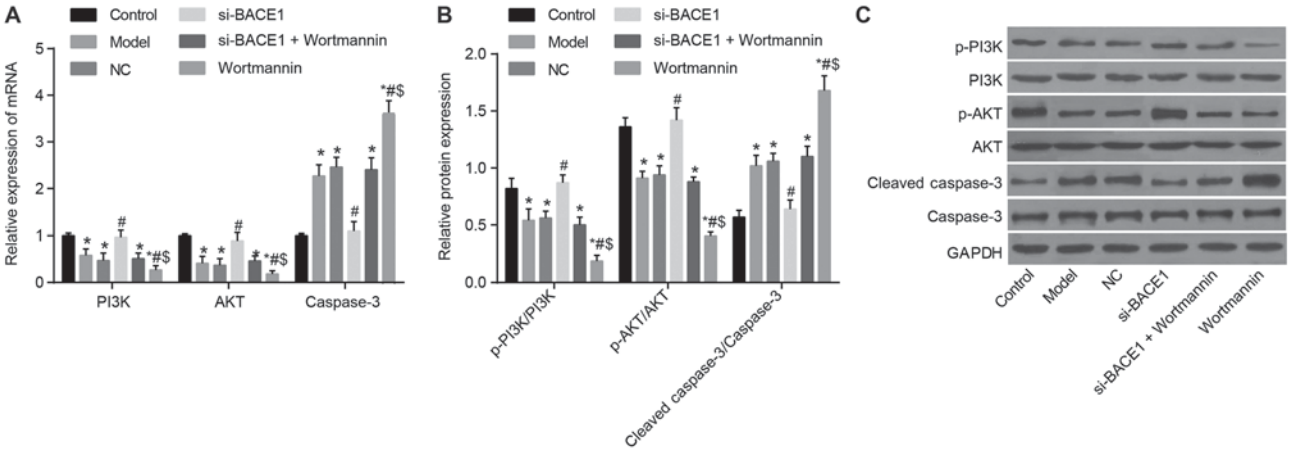

Figure 6. BACE1 gene silencing activates the PI3K/Akt signaling pathway. (A) The mRNA expression of caspase-3 was reduced, and that of PI3K and Akt was increased following reverse transcription-quantitative polymerase chain reaction. (B) The protein expression of caspase-3 was reduced, and that of PI3K and Akt was increased by silencing BACE1, (C) as determined by western blot analysis. *P<0.05 vs. the control group; #P<0.05 vs. the model group; $P<0.05 vs. the si-BACE1 + wortmannin group. NC, negative control; si-, small interfering RNA; BACE1, β-site amyloid precursor protein cleavage enzyme 1; PI3K, phosphatidylinositol-3-kinase; Akt, protein kinase B; p-, phosphorylated.

NC groups, the si-BACE1 group had a lower positive rate in the hippocampal CA1 area, and the positive rate in the wortmannin group was significantly higher. In contrast to the si-BACE1 + wortmannin group, the wortmannin group had an increased positive rate of TUNEL staining in the hippocampal CA1 region (P<0.05). There was no significant difference in the model, NC and si-BACE1 + wortmannin groups (P>0.05; Fig. 7). Consequently, the findings revealed that silencing BACE1 can activate the PI3K/Akt signaling pathway, thus inhibiting the apoptosis of hippocampal CA1 region.

Discussion

It has been suggested that at present, few satisfactory treatments for POCD are achieved and that use of anesthetics is correlated with POCD (5). However, interestingly, according to previous studies, various examples have been given to demonstrate the potential role of signaling pathways in POCD (3,6-8), indicating that studies of POCD targeting the regulation of signaling pathways might be of great importance to the development of treatments for POCD. In this study, the effects of BACE1 gene silencing on POCD after isoflurane anesthesia via the PI3K/Akt signaling pathway were studied in immature rats, and the results might provide some evidence for the improvement of POCD treatment with BACE1 gene silencing through activation of the PI3K/Akt signaling pathway and inhibition of the generation of Aβ by APP.

Initially, in this study, BACE1 gene silencing was found to activate the PI3K/Akt signaling pathway. The cleavage of the APP by enzymes, which are generally denoted as β- and γ-secretase, is a crucial process in the pathological mechanism of AD (26). BACE1, which is highly expressed in the pancreas, is an aspartyl protease that is bound to the membrane and is closely related to AD, leading to the generation of Aβ from APP (27). The inhibition of BACE1 along with acetylcholinesterase and butyrylcholinesterase plays a key role in preventing and treating AD (28). PI3K has been discovered to have an important role in regulating many cellular processes such as the survival, proliferation and differentiation of cells, and Akt is expressed as AKT1, AKT2 and AKT3 encoded separately by the PKBα, PKBβ, and PKBγ genes (29). There are multiple studies indicating that activation of the PI3K/Akt signaling pathway inhibits the growth and survival of cancer cells (29,30). Additionally, wortmannin, as a specific inhibitor of PI3K,

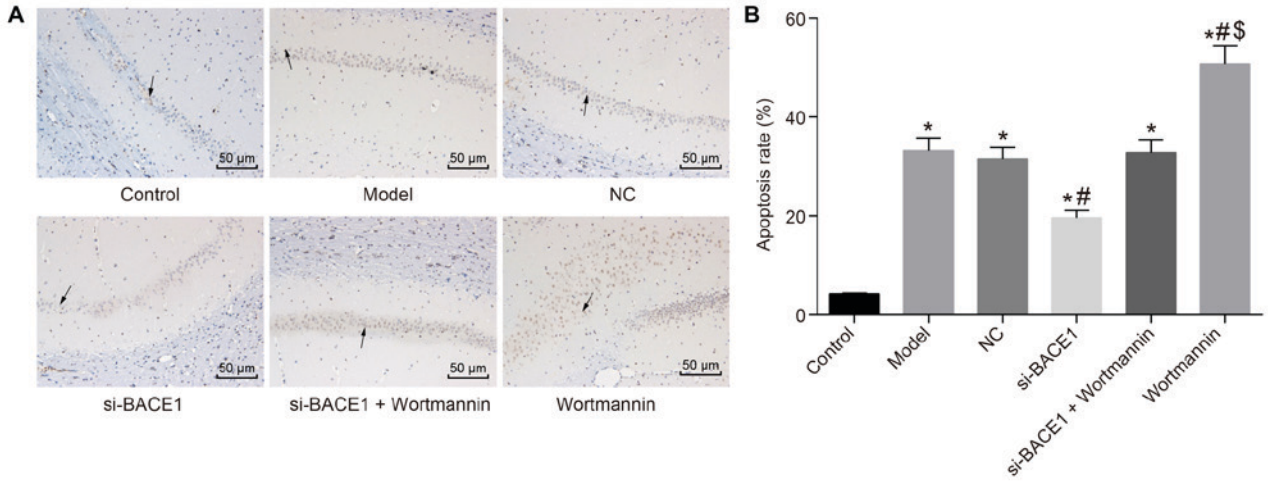

Figure 7. Silencing BACE1 promotes the activation of the PI3K/Akt signaling pathway, thereby inhibiting the apoptosis of the hippocampal CA1 region by TUNEL staining. (A) The positive rate of TUNEL staining in the rat hippocampus CA1 of the six groups; black arrows indicate apoptotic cells (magnification, x200; scale bars, 50 μm). (B) The rate of apoptosis in the hippocampal CA1 region of the six groups. *P<0.05 vs. the control group; $^{\#}$P<0.05 vs. the model group; $^{\$}$P<0.05 vs. the si-BACE1 + wortmannin group. NC, negative control; si-, small interfering RNA; BACE1, β-site amyloid precursor protein cleavage enzyme 1; PI3K, phosphatidylinositol-3-kinase; Akt, protein kinase B; TUNEL, terminal deoxynucleotidyl transferase dUTP nick-end labeling.

could decrease the expression of PI3K and Akt. All PI3Ks are suppressed by the drugs wortmannin and LY294002, of which wortmannin is a commonly used reagent in cell biology and has been applied to inhibit DNA repair, receptor-mediated endocytosis and cell proliferation (31). A previous study suggested that wortmannin, a PI3K/Akt inhibitor, decreases the inflammatory cytokines in severe acute pancreatitis (SAP) rats, demonstrating that its regulatory mechanisms may occur via the suppression of NF-κB and p38 MAPK activity (32).

Furthermore, the levels of IL-1β, IL-6, APP and Aβ in the rat hippocampus were remarkably reduced in the si-BACE1 group compared to the model group. A previous study discovered that partial inhibition of the BACE1 gene had an influence on the APP's β-cleavage to decrease the Aβ levels in the brain to improve the cognitive dysfunctions associated with AD, including implicit and explicit memory components (33). The soluble oligomers of Aβ, the main component of senile plaques in the brain, are considered to lead to the dysfunction of synapses and cognition during the early phases of AD (34,35). IL-1β, a proinflammatory cytokine, leads to neurogenic inflammation in many central nervous system diseases as well as inflammatory reaction development in the brain, and it has been revealed that POCD has a certain correlation with the concentrations of peripheral markers of inflammation, especially IL-6 and S-100β (2). In addition, IL-1β overexpression is associated with metaplasia, chronic gastritis, severe stunted growth and even an elevated risk of solid malignancy, suggesting that chronic inflammation triggers the initiation and development of cancers (36). IL-6 is a cytokine involved in the pathological mechanism of rheumatoid arthritis by its various effects on immunological and inflammatory reactions, which also plays a regulatory part in the process of metabolism, regeneration and neurons (37,38).

In addition, isoflurane caused POCD in immature rats via the regulation of IL-1β and caspase-3. It has been reported that caspase-3 is an indicator of neuronal apoptosis caused by increased expression of caspase-3 in the development of POCD (39). IL-1β is an indicator of the inflammatory response in the nervous system (40). These are two independent indicators with no direct correlation, both of which are the factors related to POCD. POCD is a type of severe neural sequela occurring after anesthesia and surgery and is associated with anesthesia duration and advanced age (41). At present, a study has reported that isoflurane can result in a significantly higher incidence of POCD (42). Chen *et al* (43), have reported that caspase-3, a regulator of neuroapoptosis induced by isoflurane, plays a negative regulatory role in the apoptosis of hippocampal neural precursor cells (NPCs) and that NPCs are related to cognition impairment. In addition, Lin *et al* (44), have confirmed that isoflurane exposure may result in POCD in rats, which has a correlation with cell damage and overexpression of inflammatory mediators in the hippocampus, induced by isoflurane. Isoflurane anesthesia has been found to increase the IL-1 level in streptozotocin-induced diabetic rat models and aggravate streptozotocin-induced cognitive impairment (45).

In conclusion, the present study reveals that BACE1 gene silencing activates the PI3K/Akt signaling pathway and inhibits the generation of Aβ by APP, thus improving POCD induced by isoflurane anesthesia in rats. The present study provides some ideas for the development of new BACE1-targeting inhibitors that can relieve the symptoms of POCD.

Acknowledgements

Not applicable.

Funding

No funding was received.

Availability of data and materials

The datasets generated and analyzed during the present study are available from the corresponding author upon reasonable request.

Authors' contributions

YBW, JQX, WL and RZZ made substantial contributions to the design of the present study. YBW, JQX, WL collated the data, and designed and developed the data in the manuscript. RZZ, SHH and YHX performed data analyses and produced the initial draft of the manuscript. All authors have read and approved the final submitted manuscript.

Ethics approval and consent to participate

All animal experimentation was approved by the Animal Ethics Committee of Lanzhou University Second Hospital (Lanzhou, China) and abided by relevant protocols.

Patient consent for publication

Not applicable.

Competing interests

The authors declare that they have no competing interests.

References

1. Jungwirth B, Zieglgansberger W, Kochs E and Rammes G: Anesthesia and postoperative cognitive dysfunction (POCD). Mini Rev Med Chem 9: 1568-1579, 2009.
2. Peng L, Xu L and Ouyang W: Role of peripheral inflammatory markers in postoperative cognitive dysfunction (POCD): A meta-analysis. PLoS One 8: e79624, 2013.
3. Ma Y, Cheng Q, Wang E, Li L and Zhang X: Inhibiting tumor necrosis factor-α signaling attenuates postoperative cognitive dysfunction in aged rats. Mol Med Rep 12: 3095-3100, 2015.
4. Ballard C, Jones E, Gauge N, Aarsland D, Nilsen OB, Saxby BK, Lowery D, Corbett A, Wesnes K, Katsaiti E, *et al*: Optimised anaesthesia to reduce post operative cognitive decline (POCD) in older patients undergoing elective surgery, a randomised controlled trial. PLoS One 7: e37410, 2012.
5. Liebert AD, Chow RT, Bicknell BT and Varigos E: Neuroprotective effects against POCD by Photobiomodulation: Evidence from assembly/disassembly of the cytoskeleton. J Exp Neurosci 10: 1-19, 2016.
6. Zhang C, Li C, Xu Z, Zhao S, Li P, Cao J and Mi W: The effect of surgical and psychological stress on learning and memory function in aged C57BL/6 mice. Neuroscience 320: 210-220, 2016.
7. Wang Y, He H, Li D, Zhu W, Duan K, Le Y, Liao Y and Ou Y: The role of the TLR4 signaling pathway in cognitive deficits following surgery in aged rats. Mol Med Rep 7: 1137-1142, 2013.
8. Hu N, Wang C, Zheng Y, Ao J, Zhang C, Xie K, Li Y, Wang H, Yu Y and Wang G: The role of the Wnt/β-catenin-Annexin A1 pathway in the process of sevoflurane-induced cognitive dysfunction. J Neurochem 137: 240-252, 2016.
9. Small DH, Mok SS and Bornstein JC: Alzheimer's disease and Abeta toxicity: From top to bottom. Nat Rev Neurosci 2: 595-598, 2001.
10. Hu N, Wang M, Xie K, Wang H, Wang C, Wang C, Wang C, Li Y, Yu Y and Wang G: Internalization of GluA2 and the underlying mechanisms of cognitive decline in aged rats following surgery and prolonged exposure to sevoflurane. Neurotoxicology 49: 94-103, 2015.
11. Hamilton DL, Findlay JA, Montagut G, Meakin PJ, Bestow D, Jalicy SM and Ashford ML: Altered amyloid precursor protein processing regulates glucose uptake and oxidation in cultured rodent myotubes. Diabetologia 57: 1684-1692, 2014.
12. He XL, Yan N, Chen XS, Qi YW, Yan Y and Cai Z: Hydrogen sulfide down-regulates BACE1 and PS1 via activating PI3K/Akt pathway in the brain of APP/PS1 transgenic mouse. Pharmacol Rep 68: 975-982, 2016.
13. Sarker D, Reid AH, Yap TA and de Bono JS: Targeting the PI3K/AKT pathway for the treatment of prostate cancer. Clin Cancer Res 15: 4799-4805, 2009.
14. Arslan F, Lai RC, Smeets MB, Akeroyd L, Choo A, Aguor EN, Timmers L, van Rijen HV, Doevendans PA, Pasterkamp G, *et al*: Mesenchymal stem cell-derived exosomes increase ATP levels, decrease oxidative stress and activate PI3K/Akt pathway to enhance myocardial viability and prevent adverse remodeling after myocardial ischemia/reperfusion injury. Stem Cell Res 10: 301-312, 2013.
15. Deng Y, Wang Z, Wang R, Zhang X, Zhang S, Wu Y, Staufenbiel M, Cai F and Song W: Amyloid-β protein (Aβ) Glu11 is the major β-secretase site of beta-site amyloid-β precursor protein-cleaving enzyme 1 (BACE1) and shifting the cleavage site to Aβ Asp1 contributes to Alzheimer pathogenesis. Eur J Neurosci 37: 1962-1969, 2013.
16. Shi X, Cai X, Di W, Li J, Xu X, Zhang A, Qi W, Zhou Z and Fang Y: MFG-E8 selectively inhibited Aβ-induced microglial M1 polarization via NF-κB and PI3K-Akt pathways. Mol Neurobiol 54: 7777-7788, 2017.
17. Chiang HC, Wang L, Xie Z, Yau A and Zhong Y: PI3 kinase signaling is involved in Abeta-induced memory loss in Drosophila. Proc Natl Acad Sci USA 107: 7060-7065, 2010.
18. Qiang W, Yau WM, Lu JX, Collinge J and Tycko R: Structural variation in amyloid-β fibrils from Alzheimer's disease clinical subtypes. Nature 541: 217-221, 2017.
19. Szaruga M, Munteanu B, Lismont S, Veugelen S, Horrè K, Mercken M, Saido TC, Ryan NS, De Vos T, Savvides SN, *et al*: Alzheimer's-causing mutations shift Aβ length by destabilizing γ-secretase-Aβn interactions. Cell 170: 443-456 e414, 2017.
20. Zhao J, Fu Y, Yasvoina M, Shao P, Hitt B, O'Connor T, Logan S, Maus E, Citron M, Berry R, *et al*: Beta-site amyloid precursor protein cleaving enzyme 1 levels become elevated in neurons around amyloid plaques: Implications for Alzheimer's disease pathogenesis. J Neurosci 27: 3639-3649, 2007.
21. Portelius E, Dean RA, Andreasson U, Mattsson N, Westerlund A, Olsson M, Demattos RB, Racke MM, Zetterberg H, May PC and Blennow K: β-site amyloid precursor protein-cleaving enzyme 1(BACE1) inhibitor treatment induces Aβ5-X peptides through alternative amyloid precursor protein cleavage. Alzheimers Res Ther 6: 75, 2014.
22. Hunt KW, Cook AW, Watts RJ, Clark CT, Vigers G, Smith D, Metcalf AT, Gunawardana IW, Burkard M, Cox AA, *et al*: Spirocyclic β-site amyloid precursor protein cleaving enzyme 1 (BACE1) inhibitors: From hit to lowering of cerebrospinal fluid (CSF) amyloid β in a higher species. J Med Chem 56: 3379-3403, 2013.
23. Mason TJ and Matthews M: Aquatic environment, housing and management in the eighth edition of the guide for the care and use of laboratory animals: Additional considerations and recommendations. J Am Assoc Lab Anim Sci 51: 329-332, 2012.
24. Livak KJ and Schmittgen TD. Analysis of relative gene expression data using real-time quantitative pcr and the 2(-Delta Delta C(T)) method. Methods 25: 402-408, 2001.
25. Tuo YL, Li XM and Luo J: Long noncoding RNA UCA1 modulates breast cancer cell growth and apoptosis through decreasing tumor suppressive miR-143. Eur Rev Med Pharmacol Sci 19: 3403-3411, 2015.
26. Holsinger RM, Goense N, Bohorquez J and Strappe P: Splice variants of the Alzheimer's disease beta-secretase, BACE1. Neurogenetics 14: 1-9, 2013.
27. Johnson JL, Chambers E and Jayasundera K: Application of a bioinformatics-based approach to identify novel putative in vivo BACE1 substrates. Biomed Eng Comput Biol 5: 1-15, 2013.
28. Kuk EB, Jo AR, Oh SI, Sohn HS, Seong SH, Roy A, Choi JS and Jung HA: Anti-Alzheimer's disease activity of compounds from the root bark of Morus alba L. Arch Pharm Res 40: 338-349, 2017.
29. Liu P, Cheng H, Roberts TM and Zhao JJ: Targeting the phosphoinositide 3-kinase pathway in cancer. Nat Rev Drug Discov 8: 627-644, 2009.
30. Engelman JA: Targeting PI3K signalling in cancer: Opportunities, challenges and limitations. Nat Rev Cancer 9: 550-562, 2009.
31. Abliz A, Deng W, Sun R, Guo W, Zhao L and Wang W: Wortmannin, PI3K/Akt signaling pathway inhibitor, attenuates thyroid injury associated with severe acute pancreatitis in rats. Int J Clin Exp Pathol 8: 13821-13833, 2015.
32. Xu P, Wang J, Yang ZW, Lou XL and Chen C: Regulatory roles of the PI3K/Akt signaling pathway in rats with severe acute pancreatitis. PLoS One 8: e81767, 2013.
33. Devi L and Ohno M: Genetic reductions of beta-site amyloid precursor protein-cleaving enzyme 1 and amyloid-beta ameliorate impairment of conditioned taste aversion memory in 5XFAD Alzheimer's disease model mice. Eur J Neurosci 31: 110-118, 2010.

34. Nishitsuji K, Tomiyama T, Ishibashi K, Ito K, Teraoka R, Lambert MP, Klein WL and Mori H: The E693Delta mutation in amyloid precursor protein increases intracellular accumulation of amyloid beta oligomers and causes endoplasmic reticulum stress-induced apoptosis in cultured cells. Am J Pathol 174: 957-969, 2009.
35. Thinakaran G and Koo EH: Amyloid precursor protein trafficking, processing, and function. J Biol Chem 283: 29615-29619, 2008.
36. Tu S, Bhagat G, Cui G, Takaishi S, Kurt-Jones EA, Rickman B, Betz KS, Penz-Oesterreicher M, Bjorkdahl O, Fox JG and Wang TC: Overexpression of interleukin-1beta induces gastric inflammation and cancer and mobilizes myeloid-derived suppressor cells in mice. Cancer Cell 14: 408-419, 2008.
37. Smolen JS, Beaulieu A, Rubbert-Roth A, Ramos-Remus C, Rovensky J, Alecock E; Woodworth T and Alten R; OPTION Investigators: Effect of interleukin-6 receptor inhibition with tocilizumab in patients with rheumatoid arthritis (OPTION study): A double-blind, placebo-controlled, randomised trial. Lancet 371: 987-997, 2008.
38. Scheller J, Chalaris A, Schmidt-Arras D and Rose-John S: The pro- and anti-inflammatory properties of the cytokine interleukin-6. Biochim Biophys Acta 1813: 878-888, 2011.
39. Miao HH, Zhen Y, Ding GN, Hong FX, Xie ZC and Tian M: Ginsenoside Rg1 attenuates isoflurane-induced caspase-3 activation via inhibiting mitochondrial dysfunction. Biomed Environ Sci 28: 116-126, 2015.
40. Cibelli M, Fidalgo AR, Terrando N, Ma D, Monaco C, Feldmann M, Takata M, Lever IJ, Nanchahal J, Fanselow MS and Maze M: Role of interleukin-1beta in postoperative cognitive dysfunction. Ann Neurol 68: 360-368, 2010.
41. Luo X, Yang L, Chen X and Li S: Tau hyperphosphorylation: A downstream effector of isoflurane-induced neuroinflammation in aged rodents. Med Hypotheses 82: 94-96, 2014.
42. Berger M, Nadler JW, Browndyke J, Terrando N, Ponnusamy V, Cohen HJ, Whitson HE and Mathew JP: Postoperative cognitive dysfunction: Minding the gaps in our knowledge of a common postoperative complication in the elderly. Anesthesiol Clin 33: 517-550, 2015.
43. Chen X, Wang W, Zhang J, Li S, Zhao Y, Tan L and Luo A: Involvement of caspase-3/PTEN signaling pathway in isoflurane-induced decrease of self-renewal capacity of hippocampal neural precursor cells. Brain Res 1625: 275-286, 2015.
44. Lin D and Zuo Z: Isoflurane induces hippocampal cell injury and cognitive impairments in adult rats. Neuropharmacology 61: 1354-1359, 2011.
45. Yang C, Zhu B, Ding J and Wang ZG: Isoflurane anesthesia aggravates cognitive impairment in streptozotocin-induced diabetic rats. Int J Clin Exp Med 7: 903-910, 2014.